A tiny gas-sensor system based on one-dimensional photonic crystal

Afaf Bouzidi, Driss Bria, Abdellatif Akjouj, Yan Pennec, Bahram Djafari-Rouhani

▶ **To cite this version:**

Afaf Bouzidi, Driss Bria, Abdellatif Akjouj, Yan Pennec, Bahram Djafari-Rouhani. A tiny gas-sensor system based on one-dimensional photonic crystal. Joint 25th Conference of the Condensed Matter Division of the European Physical Society, and 14es Journées de la Matière Condensée, CMD25-JMC14, Aug 2014, Paris, France. 10.1088/0022-3727/48/49/495102 . hal-01015253

HAL Id: hal-01015253
https://hal.science/hal-01015253

Submitted on 9 Jun 2022

HAL is a multi-disciplinary open access archive for the deposit and dissemination of scientific research documents, whether they are published or not. The documents may come from teaching and research institutions in France or abroad, or from public or private research centers.

L'archive ouverte pluridisciplinaire **HAL**, est destinée au dépôt et à la diffusion de documents scientifiques de niveau recherche, publiés ou non, émanant des établissements d'enseignement et de recherche français ou étrangers, des laboratoires publics ou privés.

Distributed under a Creative Commons Attribution - NonCommercial 4.0 International License

A tiny gas-sensor system based on 1D photonic crystal

A Bouzidi[1], **D Bria**[1,2], **A Akjouj**[2], **Y Pennec**[2] **and B Djafari-Rouhani**[2]

[1] Laboratoire de Dynamique et d'Optique des Matériaux, Département de Physique. Faculté des Sciences, Université Mohamed I, Oujda 60000, Morocco
[2] Institut d'Electronique, de Microélectronique et de Nanotechnologie (IEMN), Université de Lille1, 59655 Villeneuve d'Ascq Cedex, France

Abstract

We present a gas monitoring system for detecting the gas concentration in ambient air. This sensor is based on a 1D photonic crystal formed by alternating layers of magnesium fluoride (MgF_2) and silicon (Si) with an empty layer in the middle. The lamellar cavity (defect layer) will be filled with polluted air that has a refractive index close to that of pure air, varying between $n_0 = 1.00$ to $n_0 = 1.01$. The transmission spectrum of this sensor is calculated by the Green function approach. The numerical results show that the transmission peak, which appears in the gap, is caused by the infiltration of impure air into the empty middle layer. This transmission peak can be used for detection purposes in real-time environmental monitoring. The peak frequency is sensitive to the air-gas mixture, and a variation in the refractive index as small as $\Delta n = 10^{-5}$ can be detected. A sensitivity, $\Delta\lambda/\Delta n$, of 700 nm per refractive index unit (RIU) is achieved with this sensor.

Keywords: photonic crystals, gas-sensor, localized modes, transmission

1. Introduction

Detection of gas is a vital element in many situations such as in medical applications for monitoring and control of respiratory gases or environmental and industrial applications for controlling emissions or detecting toxic gases [1]. The global sensor market has the potential for spectacular growth due to our environmental and health concerns [2, 3]. Several types of gas sensors are available. One type, for example, measures the changes in the capacitance or in the conductance induced by the presence of certain gas atoms that are absorbed onto the surface or which diffuse into the detector material [2, 4]. Other types, known as calorimetric gas sensors, measure the variation of the temperature when certain gases pass by a heated detector [4]. But most of these methods are only applicable for specific physical properties of the gases. Recently, another class of sensor based on porous silicon technology [5–10], called an optical gas sensor, was proposed that can be applied to various gases. Among them, several papers report on the use of photonic crystals as a platform for sensor interest [11–13].

Photonic crystals are optical composite materials designed with a periodic spatial modulation of the dielectric constant at the scale of the optical wavelength [14, 15]. This type of material allows photonic band gaps (PBG) in which electromagnetic waves cannot propagate inside the crystal for any direction of the incident waves. This property makes photonic crystals extremely interesting and attractive in many physical domains [16–18]. It is now well known that the disturbance of the periodicity of the dielectric constant leads to the achievement of localized defects in the regular structure, which creates available energy levels in the photonic band gap [19, 20].

Zhao *et al* [21] made a classification of the photonic crystal gas sensors into four classes depending on the optical property used for sensing: spectroscopic absorption; surface electromagnetic wave detection; self-collimation effect; and resonance properties. The application of photonic crystals as gas sensors in the area of research seems to be very promising due to their miniaturization, high spectral sensitivity, portability, and security. Another interesting approach, based on photonic bandgap fibers (PBGF), is specifically used for the

concentration measurement of carbon dioxide [22], acetylene and hydrogen cyanide [23], or ammonia gases [24].

1D photonic crystals (1DPCs) are multilayer stacks based on alternating high- and low-refractive index materials, giving rise to high reflectivity at the position of the photonic stop band [25, 26]. 1DPCs have been currently used as a colorimetric sensor for the detection and measurement of volatile organic compounds and relative humidity [25], and detection of organic solvents [26] by a color variation due to the change in refractive index.

In this work we show that 1DPCs formed by alternating layers of magnesium fluoride (MgF_2) and silicon (Si), which contain an empty 'defect' layer in the middle can be used as an optical sensor for measuring the concentration of gases in polluted air when it is illuminated by light under normal incidence. The introduction of the cavity leads to a resonant peak inside the transmission spectrum. The objective of this paper is to discuss how to enhance the sensitivity of the peak with the variation of the refractive index of the lamellar cavity, representing the polluted air. Chen *et al* studied a 1DPC cavity in the terahertz regime and its ability to detect low concentrations of hydrogen (less than 6%) with a sensitivity of the refractive index in the range of 1.4×10^{-5} RIU [27]. We discuss theoretically the suitability of this system in the detection purpose and investigate the relative effect of the cavity thickness on the transmission peak. All transmission spectra are calculated by the Green function approach.

2. Results and discussion

Figure 1(a) represents the proposed sensor made of stacked layers containing a cavity in the middle. The analyte to be sensed is introduced into the air cavity. The light emitted by the source is detected by a spectrometer after transmission through the photonic crystal.

Figure 1(b) represents the 1D photonic structure of shape $(AB)_7$ C $(BA)_7$ used for the calculation. The periodic layers from each part of the cavity, C, are made of two materials, A and B, where A denotes the magnesium fluoride layer (MgF_2) with refractive index (RI), $n_1 = 1.37$ and thickness d_1, and B denotes the silicon layer (Si) with RI, $n_2 = 3.49$ and thickness d_2. The MgF_2 is selected owing to its low index property [28] with respect to silicon and its excellent transmission in the wavelength range of 1.4 micrometer. We designate $D = d_1 + d_2$ to be the period of the photonic crystal and C the cavity defect layer which will be filled by the analyte of RI n_0. In our study, we will keep the length of the cavity equal to the thickness of material A (d_1). It means that the cavity will be defined only by the change in its refractive index without changing the length D. The layers are assumed to be infinite along both x and y directions while the structure is finite along z. Several methods have been developed to investigate the band structures of photonic crystals as well as the transmission and/or reflection coefficients of waves which can be found elsewhere [29]. In the present paper, the study of the propagation of electromagnetic waves through the photonic band gap material is performed with the help of the interface response theory of continuous media. The objective of this theory is to calculate the Green's function of a composite system containing a large number of interfaces that separate different homogeneous media [30–32]. The results of this Green's function enables us to obtain different physical properties of the system such as the reflection and transmission coefficients of the waves.

To use the structure of figure 1 for the purpose of sensing, the common methodology is to define specific features as peaks or dips within the transmission spectrum. We know that the introduction of a cavity inside a perfect photonic crystal leads to confined resonance modes whose frequencies depend on both the thickness and the refractive index of the cavity. In the following, we will show that, at normal incidence, resonances in the transmission spectrum can occur only due to the type of material constituting the cavity with an adjustment of the size of the photonic crystal lattice parameters. Then, before going to the refractive index variation, we first discuss the occurrence of the resonances in the transmission spectrum as a function of the distance, d_1, with the objective to get a cavity mode to appear inside the band gap of the perfect photonic structure. First we present in figure 2 the photonic band structure of the perfect 1DPC composed of alternating layers of magnesium fluoride (MgF_2) and silicon (Si) with the thicknesses $d_1 = d_2 = 0.5$D. The dispersion curves are represented as a function of the dimensionless frequency $\Omega = \omega D/2\pi c$, where ω is the angular frequency (in s^{-1}), c is the velocity of light in a vacuum for the electromagnetic waves, and $k_{//}$ is the wave vector parallel to the layers. For each value of $k_{//}$, the shaded and white areas in the projected band structure correspond respectively to the minibands and the minigaps of the superlattice in which the propagation of light is respectively allowed or forbidden. The left and right panels give respectively the band structure for transverse magnetic (TM) and transverse electric (TE) polarization.

We present in figure 3 the photonic transmission spectra at normal incidence through the structure with an air-filled cavity for three different values of d_1 (0.2D, 0.5D, and 0.9D).

Figure 3(a) shows the photonic transmission curve for $d_1 = 0.2$D. One can see that, despite the existence of the air-filled cavity in the structure, the transmission curve does not present any specific features inside or outside the band gaps. When $d_1 = 0.5$D, (figure 3(b)) the transmission spectrum shows four gaps as already seen in figure 2, and a transmission peak appears in the fourth gap at the reduced frequency, $\Omega = 0.8332$. When $d_1 = 0.9$D the band gaps are wider than those obtained with $d_1 = 0.5$D (figure 2), and one peak appears in the second band gap at $\Omega = 0.5964$ (figure 3(c)).

We have shown that changing one layer of the perfect photonic crystal with another one, here MgF_2 with air, can lead to the occurrence of peaks inside different band gaps of the transmission curve. Therefore, the choice of the parameter, d_1 (or the ratio d_1/D), appears as a key parameter in the occurrence, tunability, sensitivity, and control of the cavity peak inside the band gap of the photonic crystal. It means that, for the purpose of sensing, the photonic crystal has to be carefully defined to obtain an isolated defect peak inside a band gap. This point is in close correlation with the optimization of

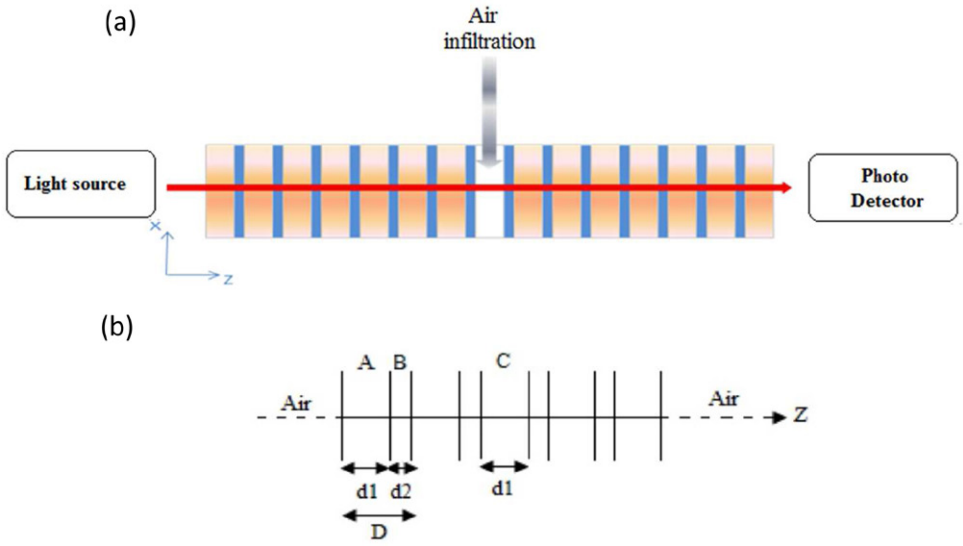

Figure 1. (a) Illustration of the photonic crystal sensor device used for the detection of a gas concentration. (b) Schematic representation of the stacked structure used for the calculation where A and B represent, respectively, the layers of magnesium fluoride (MgF_2) and silicon (Si) and C represents the infiltrated gas to be sensed.

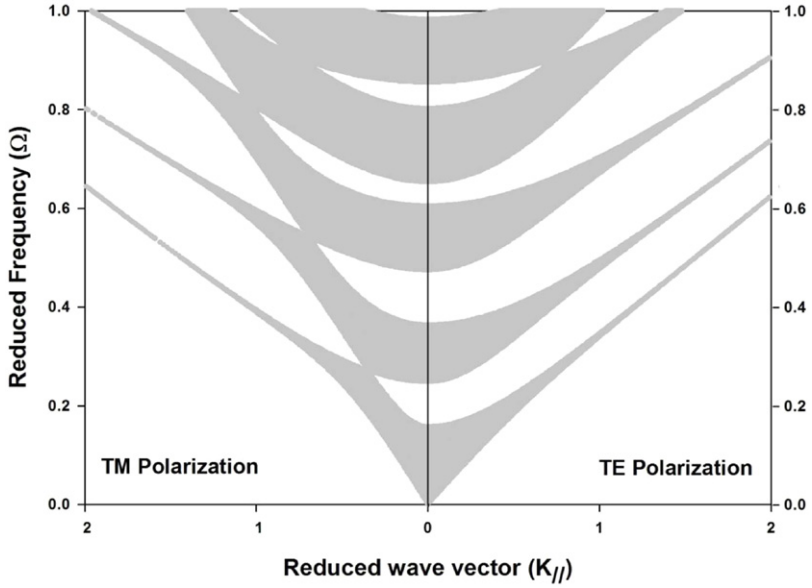

Figure 2. Projected band structure of the superlattice with thicknesses $d_1 = d_2 = 0.5$D for TE (right panel) and TM (left panel) modes. The reduced frequency, $\Omega = \omega D/2\pi$c, is presented as a function of the reduced wave vector, $k_{//}$. The shaded and white areas correspond respectively to the minibands and minigaps of the superlattice.

an efficient sensor with high sensitivity and a wide range of measurement.

To give a deeper insight into the existence and behavior of the cavity modes as a function of d_1, we have performed calculations on the evolution of the transmission of the reduced frequencies as a function of the relative length, d_1/D, in the photonic crystal containing the air defect. The results are presented in figure 4 where the grey areas represent the propagative bands containing black solid lines associated with the maxima of the transmission. In contrast, the white areas correspond to the photonic band gaps. One can see that an isolated branch can appear systematically within a band gap which frequency depends on the length, d_1. For example, for large values of d_1, ($d_1/D > 0.7$), the defect mode appears at low frequencies inside the second band gap of the structure, but when $0.6 < d_1 < 0.7$, it appears inside the third gap. In comparison with the transmission curve of figure 3(b) when $d_1/D = 0.5$, it can be confirmed that the defect mode appears in the fourth band gap. Finally, for the lower values of d_1 ($d_1 < 0.3$), the defect mode should appear at higher reduced frequencies, greater than 1, as long as the band gaps are kept open.

As a summary, one can say that we can introduce a resonant mode inside a band gap by replacing one layer of the photonic crystal with another material without introducing a geometrical defect. We can also define the order of the gap where we are seeking the defect mode. Moreover, one can tune the frequency inside one chosen band gap by carefully adapting the thickness, d_1.

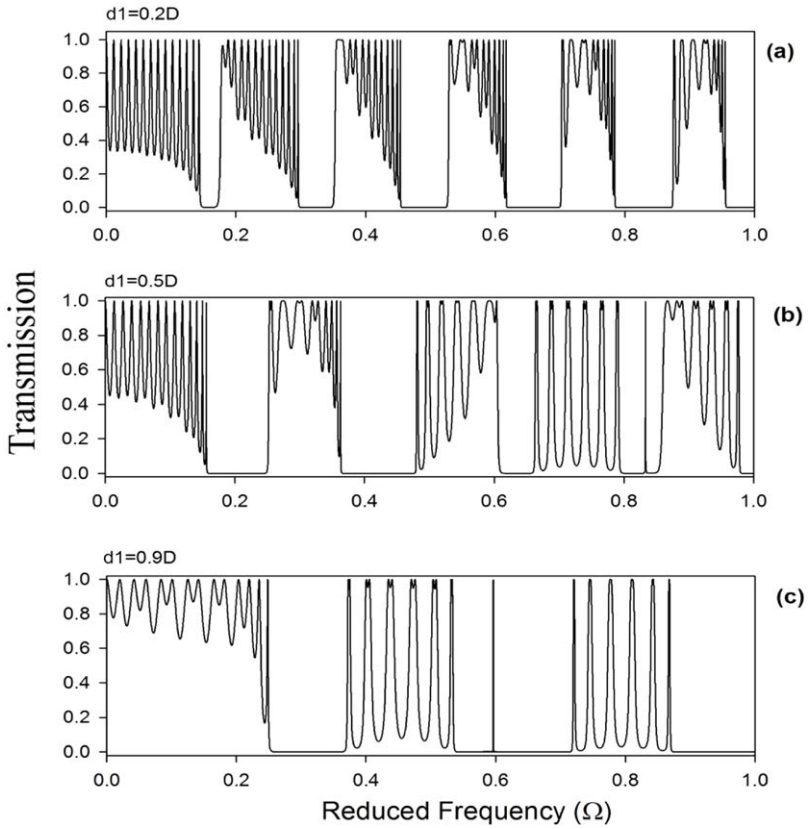

Figure 3. Photonic transmission waves through the photonic crystal of figure 1 with air-filled cavity for $d_1 = 0.2$D (a), $d_1 = 0.5$D (b), and $d_1 = 0.9$D (c) at normal incidence.

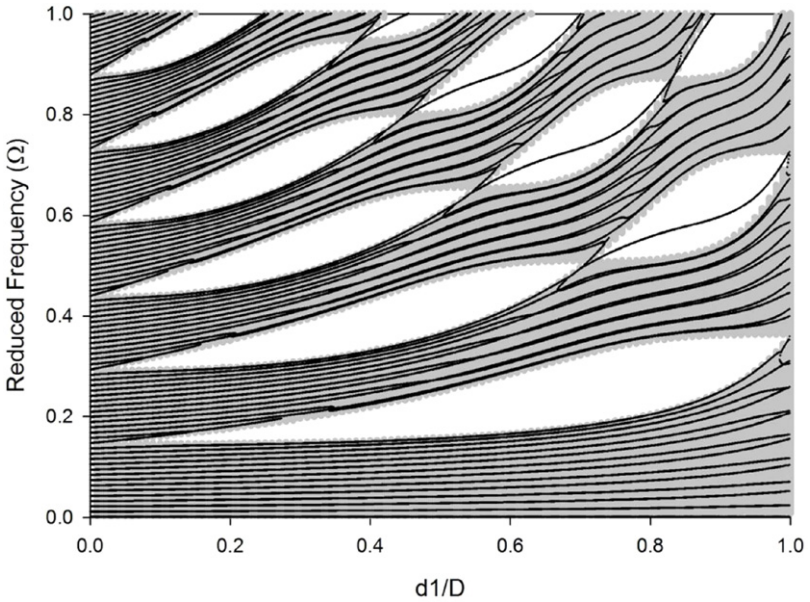

Figure 4. Variation of the transmission of the reduced frequency versus d_1 for the structure of figure 1 when the cavity is filled with air.

From a general view, to make a photonic sensor, one needs to design a structure in which the transmission coefficient displays well-defined features that are very sensitive to the infiltrating gas and relatively isolated in order to allow sensing on a sufficiently broad range of frequencies. To define the most appropriate value of the length, d_1, in such an issue, we have considered a variation of the refraction index of the cavity and we have focused our attention on the range of a larger $d_1/D > 0.7$ in which the resonant mode appears in the second band gap of the transmission curve. Figure 5 reports the evolution of the maxima of the transmitted frequencies for different orders of variation of the refractive index, i.e. $n_0 = 1.01$, $n_0 = 1.001$, and $n_0 = 1.0001$. One can see the existence of four branches corresponding to these different values of n_0.

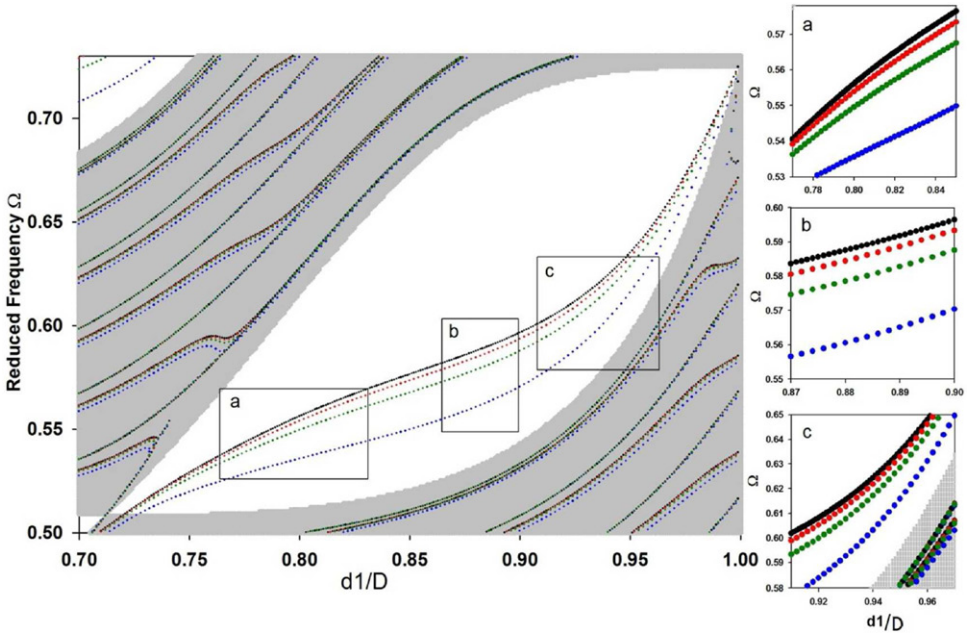

Figure 5. Variation of the maximum of the transmitted reduced frequency peak versus d_1 for the structure of figure 1 for pure air $n_0 = 1.00$ (black), and different RI of polluted air, $n_0 = 1.0001$ (red), $n_0 = 1.001$ (green), $n_0 = 1.01$ (blue), of the gas filling the cavity. The shaded and white areas, respectively, correspond to a pass and a stop band of the infinite 1D photonic crystal. The three insets (right part of the figure) correspond to the magnified areas *a*, *b*, and *c* indicated in the main figure.

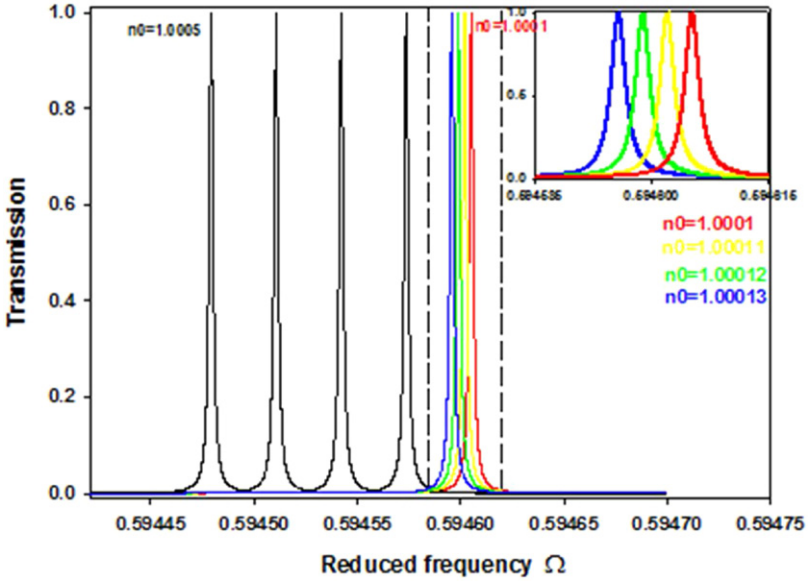

Figure 6. Normalized transmission spectra of the sensor with five different refractive indices ranging from $n_0 = 1.0001$ to $n_0 = 1.0005$ in 0.0001 increments.

These branches appear in the gap and slightly shift to the low frequencies as the refractive index increases. The relative shift in frequency between two values of the refractive index is dependent upon the value of d_1/D. To clarify this point, we have magnified the present diagram into three inserts labeled (a), (b), and (c) in figure 5. We clearly see that the higher shift in frequency is obtained for the length, d_1, belonging to domain (b), i.e. between 0.87D and 0.9D. One can note that the higher sensitivity of the mode is not obtained when the position of the peak is in the middle of the band gap, (insert (a)), as currently argued.

In the following, we give an estimation of the efficiency of the sensor, fixing the length, d_1, at 0.9D, which offers the higher sensitivity of the mode to the RI variation. We report figure 6 the evolution of the transmission curves for a variation of the RI of the polluted air with a step of 10^{-4} ($n_0 = 1.0001$ to $n_0 = 1.0005$) and show a good accuracy in the shift detection. To go further, we show that even a variation of 10^{-5} ($n_0 = 1.000\,10$ to $n_0 = 1.000\,15$) of the RI can be clearly seen as shown in the insert of figure 6. A change of 10^{-5} of the RI leads to a shift of the reduced frequency equal to 0.000 0031.

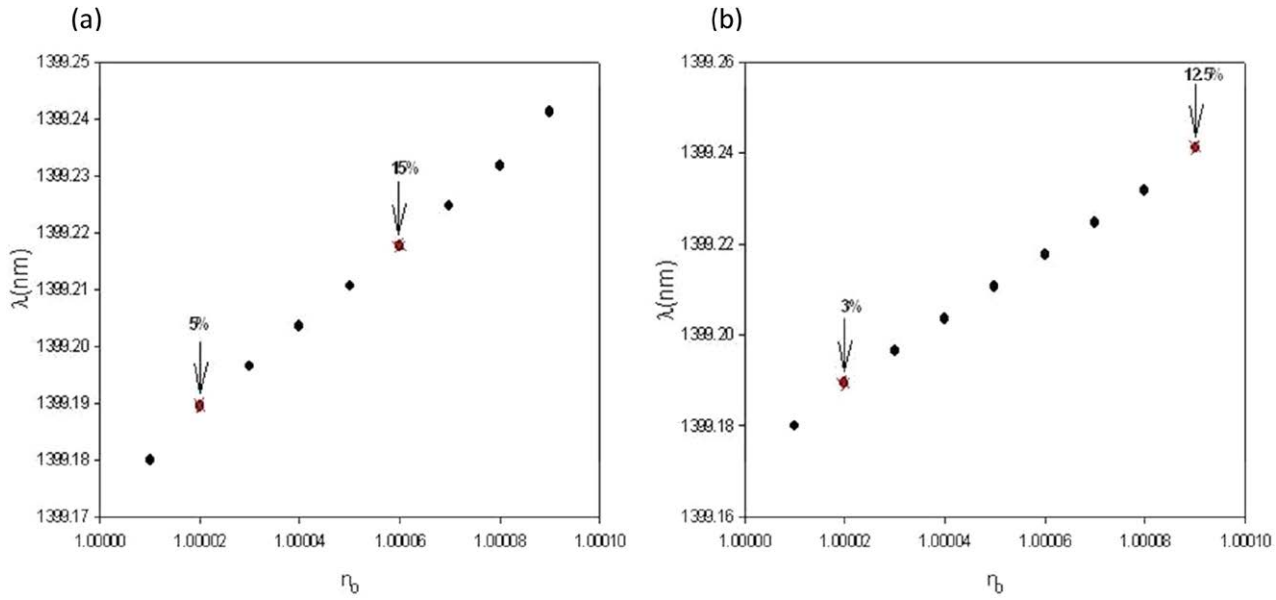

Figure 7. Resonant wavelength, λ, plotted as a function of polluted air highlighting two different concentrations of (a) methane in air and (b) ethane in air.

Table 1. Refractive index n_{mix} of methane in air at different concentrations [33].

Methane	C_{CH4}	C_{air}	n_{mix}
5%	0.05	0.95	1.000 0222
15%	0.15	0.85	1.000 0666

Table 2. Refractive index n_{mix} of ethane in air at different concentrations [33].

Ethane	C_{CH4}	C_{air}	n_{mix}
3%	0.03	0.97	1.000 0228
12.5%	0.125	0.875	1.000 095

In the following, we have applied the above analysis to a practical situation, fixing the lattice parameter of the photonic sensor to $D = 832$ nm with $d_1 = 0.9$D. With these parameters, the working wavelength of the sensor will be close to the infrared (IR) spectrum with a wavelength of the resonant mode associated with the air cavity equal to 1395.03 nm. In this spectral domain, the sensitivity of the sensor, defined by $S = \Delta\lambda/\Delta n$, is estimated to be 700 nm/RIU. Then, we calculate the response of the sensor in the detection of polluted air constituted with different concentrations of methane and ethane where the corresponding RIs are reported in tables 1 and 2 from [33].

Figure 7 represents the dependence of the wavelength, λ, of the optical resonance versus the RI for polluted air with methane (figure 7(a)) and ethane (figure 7(b)) at different concentrations filling the cavity. One can see that the wavelength varies linearly with the RI where the slope represents the sensitivity of 748 nm/RIU. It remains that a variation of the concentration of 2.5% (respectively 1.35%) of methane (respectively ethane) in air can be detectable.

This sensor is used for monitoring the level of gas concentration in ambient air. Gas mixtures can also be detected by Calorimetric methods [26].

Table 3. The sensitivity calculations for three different structures.

Structure	S (nm/RIU)	Q	FoM (RIU^{-1})
$(AB)_7$ C $(BA)_7$	706	300 000	149 000
$(AB)_6$ C $(BA)_6$	706	48 580	24 000
$(AB)_5$ C $(BA)_5$	706	8880	4500

The most common way to estimate the efficiency of a sensor is to calculate its sensitivity given by the following expression:

$$S = \frac{\Delta\lambda}{\Delta n} \text{ (nm/RIU)}.$$

The sensor also needs to have high transmission efficiency and a high Q factor, which could make the detection easy and feasible. The Q factor is defined as$\omega_0/\Delta\omega$, where $\Delta\omega$ is the full width at half-maximum (FWHM) of the resonator's Lorentzian response and ω_0 is the resonance frequency [10].

The sensing performance of photonic structures can also be characterized by the figure of merit, FoM $= S/\Delta\lambda$. This formula indicates that narrow resonances are improve sensing applications since they allow an accurate determination of the resonance shift with changes in the environment by monitoring the transmittance at a wavelength close to resonance [34].

For comparison, we summarize in table 3 the sensitivity calculations for three different structures: $(AB)_7$ C $(BA)_7$ presented in this work, $(AB)_6$ C $(BA)_6$, and $(AB)_5$ C $(BA)_5$.

The value of the Q factor of the structure $(AB)_7$ C $(BA)_7$, equal to 300 000, is on the same order as those reported in the literature. Sünner *et al* reached a Q factor of 380 000 with a PhC resonator based on a modulation of the hole radii along a waveguide [14]. Amoudache *et al* [17] reported another type of sensor in which the simultaneous control of optical and acoustic modes can be used for sensing purposes. In their paper the optical quality factor Q is about 4000, the sensitivity about 58 nm/RIU, and a figure of merit equal to 175 RIU^{-1}.

Until now, we studied the structure without introducing any geometrical defect, which means that the cavity thickness was set equal to the thickness, d_1. We now introduce a geometrical defect by increasing the width of the cavity from $d_0 = 0.9$D, to $d_0 = 1.0$D then to $d_0 = 2.0$D. For $d_0 = 1.5$D, a change of 10^{-5} of the RI leads to a shift of the reduced frequency equal to 0.000 0057, and for $d_0 = 2$D the reduced frequency shift reaches 0.000 0015. We note that changing the thickness, $d_0 = d_1 = 0.9$D, to $d_0 = 1.5$D, increases the sensitivity of the sensor to $S = 900$ nm/RIU. Different geometrical shapes of the cavity, including tapered cavities for example, open the way to higher optimization of the sensitivity of the sensor.

3. Conclusion

In summary, we have studied the application of a 1D photonic crystal cavity formed by alternating layers of magnesium fluoride (MgF_2) with thickness d_1 and silicon (Si) with thickness d_2. We show that this structure can be used as a highly sensitive gas sensor for measuring the concentration of a gas in air when it is illuminated by light in normal incidence. This goal is reached by measuring the spectral response of the cavity with respect to the environmental refractive index. We have shown that a resonant mode can be introduced inside the band gap by changing the MgF_2 layer of the medium by the air without introducing a geometrical defect. Also, we can define the order of the gap and then the frequency, where we would like to see the appearance of the defect mode depending on the choice of d_1 and, thus, d_1/D. The thickness of the defect layer can be tuned to design a structure in which the modes inside the transmission spectra are well-defined and sufficiently isolated. This sensor offers high sensitivity of the mode to the refractive index variation—a variation of 10^{-5} of the refractive index can be clearly detectable. This device has the additional advantage of being able to monitor the environment at normal conditions and in real-time. Finally, it should be noted that the sensitivity of this structure can be improved by changing the size of the defect layer in the structure. This system could be employed for monitoring in the environmental field, for detection of dangerous and/or air polluting gas concentrations, and for liquid analysis (water analysis), as well as in the medical sector.

References

[1] Feng C, Feng G Y, Zhou G R, Chen N J and Zhou S H 2012 *Laser Phys. Lett.* **9** 875

[2] Pergande D, Geppert T M, Rhein A V, Schweizer S L, Wehrspohn R B, Moretton S and Lambrecht A 2011 *J. Appl. Phys.* **109** 083117

[3] Dorfner D, Zabel T, Hürlimann T, Hauke N, Frandsen L, Rant U, Abstreiter G and Finley J 2009 *Biosens. Bioelectron.* **24** 3688

[4] Geppert T M *et al* 2004 *Proc. SPIE* **5511** 61

[5] Zangooie S, Bjorklund R and Arwin H 1997 *Sensors Actuators* B **43** 168

[6] Gao J, Gao T and Sailor M J 2000 *Appl. Phys. Lett.* **77** 901

[7] Abdelghani A, Chovelon J M, Jaffrezic-Renault N, Lacroix M, Gagnaire H, Veillas C, Berkova B, Chomat M and Matejec V 1997 *Sensors Actuators* B **44** 495

[8] Oton C J, Pancheri L, Gaburro Z, Pavesi L, Baratto C, Faglia G and Sberveglieri G 2003 *Phys. Status. Solidi. a* **197** 523

[9] Mulloni V and Pavesi L 2000 *Appl. Phys. Lett.* **76** 2523–5

[10] Snow P A, Squire E K, St. J. Russell P and Canham L T 1999 *J. Appl. Phys.* **86** 1781

[11] Wang X, Xu Z, Lu N, Zhu J and Jin G 2008 *Opt. Commun.* **281** 1725

[12] Dündar M A, Ryckebosch E C I, Nötzel R, Karouta F, Van IJzendoorn L J and Van Der Heijden R W 2010 *Opt. Express* **18** 4049

[13] Liu Y and Salemink H W M 2012 *Opt. Express* **20** 19912

[14] Sünner T, Stichel T, Kwon S-H, Schlereth T W, Höfling S, Kamp M and Forchel A 2008 *Appl. Phys. Lett.* **92** 261112

[15] Banerjee A 2009 *Prog. Electromagn. Res.* **89** 11–22

[16] Lucklum R, Zubtsov M and Oseev A 2013 *Anal. Bioanal. Chem.* **405** 6497

[17] Amoudache S, Pennec Y, Djafari Rouhani B, Khater A, Lucklum R and Tigrine R 2014 *J. Appl. Phys.* **115** 134503

[18] Bria D, Assouar M B, Oudich M, Pennec Y, Vasseur J and Djafari-Rouhani B 2011 *J. Appl. Phys.* **109** 014507

[19] Dahdah J, Courjal N and Baida F I 2010 *J. Opt. Soc. Am.* B **27** 305–10

[20] Wang X, Tan Q, Yang C, Lu N and Jin G 2012 *Optik* **123** 2113

[21] Zhao Y, Zhang Y and Wang Q 2011 *Sensors Actuators* B **160** 1288

[22] Pawłat J, Li X, Sugiyama T, Matsuo T, Zimin Y and Ueda T 2010 *Solid State Phenom.* **165** 316

[23] Ritari T, Tuominen J, Ludvigsen H, Petersen J C, Sørensen T, Hansen T P and Simonsen H R 2004 *Opt. Express* **12** 4080

[24] Pawlat J, Sugiyama T, Matsuo T and Ueda T 2007 *Plasma Process. Polym.* **4** 743

[25] Dou Y, Han J, Wang T, Wei M, Evans D G and Duan X 2012 *J. Mater. Chem.* **22** 14001

[26] Wang Z *et al* 2011 *J. Mater. Chem.* **21** 1264

[27] Chen T, Han Z, Liu J and Hong Z 2014 *Appl. Opt.* **53** 3454

[28] Bruynooghe S, Tonova D, Sundermann M, Koch T and Shulz U 2015 *Surf. Coat. Technol.* **267** 40–4

[29] Lucklum R and Li J 2009 *Meas. Sci. Technol.* **20** 124014

[30] Bah M L, Akjouj A, El Boudouti E H, Djafari-Rouhani B and Dobrzynski L 1996 *J. Phys.: Condens. Matter* **8** 4171

[31] Mir A, Akjouj A, El Boudouti E H, Djafari-Rouhani B and Dobrzynski L 2001 *Vacuum* **63** 197

[32] Bria D, Djafari-Rouhani B, El Boudouti E H, Mir A, Akjouj A and Nougaoui A 2002 *J. Appl. Phys.* **91** 2569

[33] Passaro V M N, Troia B and De Leonardis F 2012 *Sensors Actuators* B **168** 402

[34] Offermans P, Schaafsma M C, Rodriguez S R K, zhang Y, Crego-Calama M, Brongersma S H and Rivas J G 2011 *ACS Nano* **5151**